Wave interaction in relativistic harmonic gyro-traveling-wave devices

R. Ngogang, G. S. Nusinovich, T. M. Antonsen, Jr., and V. L. Granatstein
Institute for Research in Electronics and Applied Physics, University of Maryland, College Park, Maryland 20742-3511, USA
(Received 10 November 2005; published 3 May 2006)

In gyro-traveling-wave devices, several waves can be excited at different cyclotron harmonics simultaneously. This paper analyzes the interaction between three waves synchronous with gyrating electrons at different cyclotron harmonics in two relativistic gyro-amplifier configurations; viz., gyro-traveling-wave tubes and gyrotwystrons. Two types of nonlinear interactions are considered: (a) excitation of two waves at cyclotron harmonics by a wave excited at the fundamental resonance, and (b) excitation of a wave at the fundamental resonance and another wave at the third harmonic by a wave excited at the second cyclotron harmonic. The effect of the overlapping of electron cyclotron resonances on the performance of relativistic gyrodevices is investigated as well.

DOI: 10.1103/PhysRevE.73.056401 PACS number(s): 52.35.Mw, 84.40.Ik, 41.60.Cr, 84.40.Fe

I. INTRODUCTION

Interaction between three or four waves in nonlinear media is a topic extensively studied in the physics of plasmas [1,2], nonlinear optics [3,4], and parametric systems [5]. Such an interaction takes place when the wave frequencies ω and wave vectors $\vec{k}$ obey the synchronism conditions. For three-wave interaction these conditions have the form:

$$\omega_1 + \omega_2 = \omega_3, \quad \vec{k}_1 + \vec{k}_2 = \vec{k}_3. \tag{1}$$

In the sources of coherent electromagnetic (EM) radiation driven by electron beams such a wave interaction occurs due to the presence of an electron beam which can be treated as an active nonlinear medium. This active medium may not necessarily be active enough to excite all three waves in the small-signal regime. It may happen that some of these waves can be excited due to nonlinear interaction between the waves only. In such a case a so-called decay process may take place when an initially excited wave then gives rise to others.

Since a beam excites the waves of a microwave circuit (waveguide) the wave frequencies and axial wave numbers obey the waveguide dispersion equation. This equation is especially simple for standard waveguides used in gyro-traveling-wave tubes (gyro-TWTs) because these tubes usually operate as fast-wave devices [6]:

$$\omega^2 = \omega_{cut}^2 + c^2 k_z^2. \tag{2}$$

In (2) ω_{cut} is the cutoff frequency of a waveguide, k_z is the axial wave number, and c is the speed of light.

The operation of gyrodevices is based on the cyclotron resonance between Doppler shifted EM waves and electrons gyrating in the external magnetic field:

$$\omega - k_z v_z \approx s\Omega. \tag{3}$$

Here, Ω and v_z are the cyclotron frequency and axial velocity of electrons, s is the resonant number of the cyclotron harmonic. The width of the cyclotron resonance band is inversely proportional to the number of electron orbits in the interaction space, N (see, e.g., [7]), which is typically large enough, $N \gg 1$. Therefore, the three-wave interaction determined by the condition (1) may take place only for waves resonant with different cyclotron harmonics, while the four-wave interaction determined by similar conditions and analyzed elsewhere [8] may take place in the case of all waves synchronous with the same cyclotron harmonic.

In gyro-TWTs with cylindrical waveguides the synchronism condition for the wave vectors (1) can be rewritten as

$$m_1 + m_2 = m_3, \tag{4}$$

and

$$k_{1z} + k_{2z} \approx k_{3z}. \tag{5}$$

In (4) m_s are azimuthal indices of nonsymmetric waves rotating in a circular waveguide.

The condition of synchronism between axial wave numbers (5) is absent in gyrotron oscillators, which operate at frequencies close to cutoff. In gyro-TWTs, as follows from (2), this condition together with the cyclotron resonance condition (3) can be fulfilled only for some specific waves. To illustrate this important statement, consider the dispersion diagram shown in Fig. 1 for symmetric TE_{01}, TE_{02}, and TE_{03}-waves, which can be in cyclotron resonance with gyrating electrons at the fundamental, second, and third cyclotron harmonics, respectively. Assume that the first wave is excited by a signal at frequency ω_s. Then, in an amplifier, two other waves should be excited at $2\omega_s$ (TE_{02}-wave) and $3\omega_s$ (TE_{03}-wave). These frequencies are shown in Fig. 1 by dotted horizontal lines. As one can see, the intersection of these lines with dispersion curves for the waveguide modes takes place at a certain distance from the straight lines showing the cyclotron resonance at corresponding harmonics. This departure from the exact cyclotron resonance, of course, should weaken the excitation of second and third waves. The analysis of this effect is one of the main topics of our study.

Note that alternatively, in multistage gyro-amplifiers, operation in frequency-multiplying regimes is possible. In such devices, the beam can be modulated in the input stage (cavity or waveguide) by an external signal at the frequency ω_s. Then, in the drift section separating the input and output stages of the device, this modulation gives rise to high-frequency components in electron current density not only at

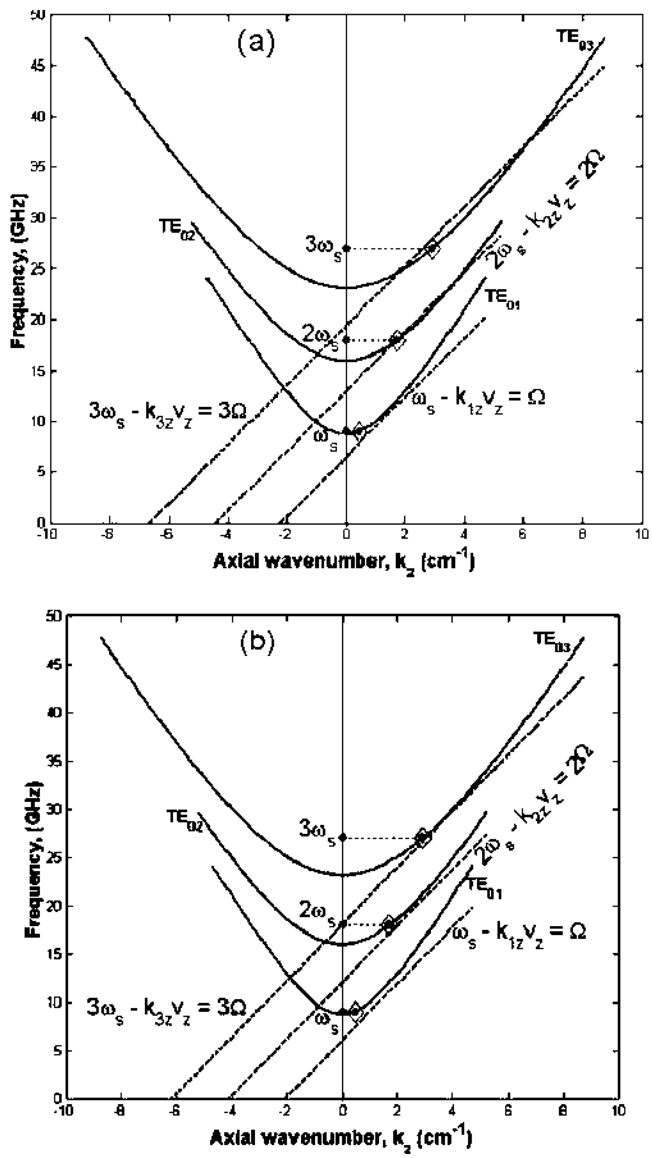

FIG. 1. Dispersion diagram when the magnetic field is optimal for the fundamental harmonic (a) and the second harmonic (b) interaction: diamonds indicate the operating points for all three waves at corresponding harmonics of the signal frequency.

ω_s, but also at its harmonics. As a result, the output stage of such a device can operate at harmonics of ω_s [9]. In terms of the dispersion diagrams shown in Fig. 1(a), this means that one can tune the external magnetic field to provide, for example, the most efficient interaction in the output waveguide with the TE$_{02}$-wave at the second cyclotron harmonic. Then, the departure from exact cyclotron resonance will take place at the TE$_{01}$- and TE$_{03}$-waves [Fig. 1(b)].

Our study will be focused on the analysis of such interaction between the waves in two configurations of gyro-amplifiers, viz., the gyro-TWT and the gyrotwystron. The latter device consists of an input cavity and an output waveguide separated by a drift section and, hence, combines the merits of klystrons (high gain) and traveling-wave tubes (large bandwidth). We will consider the operation of these devices driven by relativistic electron beams that is motivated in part by development of relativistic gyro-amplifiers for future linear colliders [10]. In high-power relativistic gyro-amplifiers, the amplitude of the EM field acting on gyrating electrons can be so large that cyclotron resonances at neighboring harmonics can overlap. This effect and corresponding stochasticity of electron orbits was recently analyzed in [11]. In the present paper we analyze the effect of this overlapping on the wave interaction.

The paper is organized as follows: Sec. II contains a qualitative theory explaining the mechanism of nonlinear wave interaction in gyrodevices. Then, in Sec. III we describe the formalism used in our study. (Details are given in the Appendix.) Results of the study of gyro-TWTs and gyrotwystrons in the absence of resonance overlapping are given in Sec. IV, and the effects of overlapping on this interaction are discussed in Sec. V. In Sec. VI we discuss the applications of the results obtained to possible realistic systems. Finally, Sec. VII summarizes this work.

II. QUALITATIVE THEORY

To illustrate the physical nature of interaction between the waves resonant with electrons at different cyclotron harmonics, we can consider a very simple model, a two-wave interaction. Indeed, the two-wave interaction can be considered as a degenerate case of the three-wave interaction determined by (1) assuming that in (1) the frequency and the wave vector of the first and second waves are equal; thus (1), (4), and (5) reduce to

$$2\omega_1 = \omega_2, \quad 2m_1 = m_2, \quad 2k_{1z} = k_{2z}. \tag{6}$$

Here, we replaced the index of the third wave in (1), (4), (5) by the index "2". Assume also that the waveguide has strong end reflections and, therefore, each wave is a standing wave formed by two traveling waves bouncing back and forth, and electrons are in resonance with the forward traveling waves only. Since these strong reflections form a resonator from this waveguide, the amplitudes of these standing waves, in the nonstationary regimes, can depend on time.

In such formulation, the problem becomes similar to the analysis of parametric instabilities in gyrotron oscillators carried out in [12,13]. The only difference between the formalism developed in [12,13] and our model is that in [12,13] it was considered the interaction of gyrating electrons with the modes having an arbitrary axial structure, while in our case electrons interact with forward waves; hence the axial structure should be given as $\exp(-ik_z z)$. To describe the wave interaction at a qualitative level, one can solve these equations of motion by the method of successive iterations assuming that the amplitudes of modes are small enough and, hence, cause small perturbations in electron motion. (This method used for gyrotron oscillators in [8,12] is essentially the same as the one used in the theory of optical masers [14] and nonlinear optics [4].) Assume also that we consider an ideal electron beam with no velocity spread. Since in calculating the source terms responsible for the excitation of EM fields in a cylindrical waveguide by an electron beam, the $\vec{j}\vec{E}_s^*$ product characterizing the interaction of an electron filament with the field of the sth mode should be averaged over initial gyrophases and over all azimuthal coordinates of electron guiding centers, only a few perturbation terms will be left after double averaging. Then, the resulting equations can be written for two typical cases obeying the first two conditions (6) in the following way:

Case 1. An electron beam excites the first wave at the fundamental cyclotron resonance, and this wave in the process of wave interaction can excite the second wave resonant with the second cyclotron harmonic. Such a problem has a certain relevance to the generation of harmonics of the signal frequency in gyro-TWTs that is the problem extensively studied in linear-beam TWTs [15]. Corresponding simplified equations for mode amplitudes can be given as [12] follows:

$$\frac{dA_1}{dt} = A_1(\sigma_1 - \beta_1 A_1^2),$$

$$\frac{dA_2}{dt} = q(-\sigma_2 A_2 - A_1^2 \cos \alpha),$$

$$\frac{d\alpha}{dt} = \delta - q\frac{A_1^2}{A_2} \sin \alpha. \tag{7}$$

Here we ignored the effect of the second wave on the first wave, but took into account the effect of the first wave on the second one; σ_1 and σ_2 are the increment of the first and the decrement of the second modes, respectively, β_1 describes the self-saturation of the first mode, q is the ratio of the coupling impedances of these modes to the beam and $\delta \propto \omega_2 - 2\omega_1$ is the frequency mismatch. As follows from (7), the stable oscillations of the first mode with the intensity $A_1^2 = \sigma_1/\beta_1$, due to the mode interaction, can be accompanied with oscillations of the second mode: $A_2 = A_1^2/\sqrt{\sigma_2^2 + (\delta/q)^2}$, $\tan \alpha = \delta/q\sigma_2$. As the frequency mismatch δ increases, the amplitude of these oscillations decreases.

Case 2. An electron beam excites the second mode resonant with the second cyclotron harmonic, and this mode, in turn, due to the mode interaction process, supports oscillations of the first mode resonant with the fundamental cyclotron frequency. This problem is relevant to the design of gyro-TWTs operating at the second cyclotron harmonics where some parasitic traveling waves can be excited at the fundamental cyclotron resonance. Corresponding equations can be given as [12] follows:

$$\frac{dM_1}{dt} = -2M_1(1 - A_2 \sin \alpha),$$

$$\frac{dA_2}{dt} = A_2(\sigma - \beta A_2^2) - 2M_1 \sin \alpha,$$

$$\frac{d\alpha}{dt} = -\delta + \left(2A_2 - \frac{M_1}{A_2}\right)\cos \alpha. \tag{8}$$

Here $M_1 = A_1^2$ is the intensity of the first mode excited at the fundamental cyclotron resonance. In the absence of self-saturation effects in the dynamics of the second mode ($\beta \to 0$), Eqs. (8) are reduced to those studied in Ref. [16], where it was shown that such a simple set of equations can exhibit an interesting sequence of pitchfork bifurcations resulting in the onset of chaotic oscillations. After these introductory remarks and examples we can move to the formulation of the problem under study.

III. FORMALISM

We consider here an ideal beam of relativistic electrons (velocity spread is not taken into account) gyrating in a constant magnetic field and interacting with traveling fast EM waves in a cylindrical structure. The self-consistent set of equations describing electron motion and the wave excitation are very similar to those derived in Refs. [7] and [17]. These equations hold for both the gyrotwystron and the gyro-TWT since they both employ a waveguide, although the boundary conditions at the waveguide entrance are different.

Let us start from equations describing the excitation of waves, which obey conditions (4) and (5). The electric field can be represented as a superposition of transverse electric ($\mathrm{TE_{mp}}$) modes:

$$\vec{E} = \mathrm{Re}\left\{\sum_s A_s(z,t)\vec{E}_s(\vec{r}_\perp)e^{i(\omega_s t - k_{sz}z)}\right\}. \tag{9}$$

For simplicity the index s instead of m,p is used to label the modes. In (9), $A_s(z,t)$ is the complex amplitude of the mode labeled s, $\vec{E}_s$ describes the transverse structure of this mode in a waveguide of length L, k_{sz} is its axial wave number, and ω_s is the mode frequency. Assume that the axial wave number obeys the condition

$$\pi/L \ll k_{sz} \ll \omega_s/c, \tag{10}$$

the left part of which ($\pi/L \ll k_{sz}$) implies that one can neglect electron interaction with the nonresonant backward wave (proportional to $\exp\{i(\omega_s t + k_{sz}z)\}$), while the right part ($k_{sz} \ll \omega_s/c$) allows one to ignore the changes in electron axial momentum in the process of interaction [6,7]. Since the complex amplitude, $A_s(z,t)$, in (9) is a slowly varying function of time ($|dA_s/dt| \ll \omega_s A_s$), one can readily derive from Maxwell equations the following envelope equation for the mode amplitudes:

$$\frac{\partial A_s}{\partial z} + \frac{1}{v_{gr_s}}\frac{\partial A_s}{\partial t} = \frac{-4\pi\omega_s}{c^2 N_s k_{sz}}\left\langle\left\langle \int_{s_\perp} \vec{j}_{\omega_s\perp} \cdot \vec{E}_s^* e^{ik_{sz}z} ds_\perp \right\rangle\right\rangle, \tag{11}$$

where, N_s is the norm of the wave given by

$$N_s = \frac{c}{4\pi}\int_{s_\perp} |\vec{E}_s|^2 ds_\perp. \tag{12}$$

In (11), the double brackets, $\langle\langle \cdots \rangle\rangle$, denote averaging over the wave period and over the electron entrance phases, v_{gr_s} is the wave group velocity, and $\vec{j}_{\omega_s\perp}$ is the transverse component of the high frequency current density

$$\vec{j} = \mathrm{Re}\{\vec{j}_{\omega_s}\exp(i\omega_s t)\}. \tag{13}$$

The components of the transverse electric field $\vec{E}_s$ can be expressed via the Hertz potential Ψ, which satisfies the membrane equation $\Delta_\perp \Psi + k_\perp^2 \Psi = 0$ with the boundary condition that the normal derivative of Ψ at the wall vanishes. The spatial dependence of the EM field for a cylindrical waveguide can be written as follows:

$$\vec{E}_s = \frac{k_s}{k_{s\perp}^2}\left[\frac{1}{r}\frac{\partial \Psi}{\partial \theta}\hat{r} - \frac{\partial \Psi}{\partial r}\hat{\theta}\right]. \qquad (14)$$

As shown elsewhere [7,18], the membrane function of the field acting upon electrons gyrating in an external magnetic field with the electron cyclotron frequency Ω and Larmor radius $a = v_\perp / \Omega$ can be represented as $\Psi = \sum_l J_l(k_{s\perp} a) L_l \times \exp(-il\theta)$. Here the Bessel function $J_l(k_{s\perp}a)$ describes the amplitude of the lth order multipole responsible for interaction at the lth cyclotron harmonic. The operator L_l describes the transverse structure of the rf Lorentz force acting on electrons with transverse polar coordinates of the electron guiding center R_0, φ_0. For cylindrical waveguides

$$L_l = J_{(l\mp m)}(k_{s\perp} R_0)\exp[i(l \mp m)\varphi_0]. \qquad (15)$$

The index l indicates the number of the resonant cyclotron harmonic ($\omega \approx 1\Omega$), m is the azimuthal index of the wave. The index $l-m$ is used when the azimuthal rotation of the wave in the cylindrical waveguide is in the same direction, as the direction of rotation of the electron in the external magnetic field, $l+m$ corresponds to the case of rotation in opposite directions.

In relativistic gyro-amplifiers, when the wave amplitudes are large the cyclotron resonances at different harmonics can overlap. Then, as shown in Ref. [19], Eq. (11), with the use of (13)–(15) can be reduced to

$$\frac{\partial F_s}{\partial \xi} + \frac{1}{\beta_{grs}}\frac{\partial F_s}{\partial t'} = -I_s \frac{1}{2\pi}\int_0^{2\pi} p_\perp e^{-i(\omega_s t - k_{sz} z)}[b_1 J_s'(\hat{a}_s)e^{i\theta} + b_2 J_2'(\hat{a}_s)e^{i2\theta} + b_3 J_3'(\hat{a}_s)e^{i3\theta}]d\theta_0. \qquad (16)$$

In (16), $\xi = \omega_s z / c\beta_{z_0}$ is the normalized axial coordinate, $t' = \omega_s t / \beta_{z_0}$ is the normalized time variable, and θ is the electron gyro-phase with an initial value θ_0. Also, $F_s = eA_s L_s / m_0 c \omega_s$ is the normalized field amplitude, and $b_{1,2,3} = |L_{1,2,3}/L_s|$ is the ratio of the coupling impedances of electrons to the wave at different cyclotron harmonics. Note that one of the b parameters (the one, which corresponds to the dominant cyclotron resonance for a given wave) is equal to unity, $b_s = 1$. The Bessel function argument is given by $\hat{a}_s = k_{s\perp} a = k_{s\perp} c\beta_{\perp s}/\Omega = \kappa_s p_\perp / \mu$, where $\mu = \Omega_0 / \omega_s$ is the ratio of the initial cyclotron frequency to the signal frequency. The upper prime means the derivative of Bessel functions. The electron momentum components are normalized to $mc\gamma_0$ (γ_0 is the initial electron energy normalized to the rest energy), β_{gr_s} is the group velocity, v_{gr_s}, normalized to the speed of light: $\beta_{gr_s} = v_{gr_s}/c = ck_{sz}/\omega_s$. The normalized current parameter I_s is defined as

$$I_s = 4\frac{eI_b}{m_o c^3}\frac{\kappa_s^2 J_{m-s}^2(k_{s\perp}R_0)}{h_s(\nu^2 - m^2)J_m^2(\nu)}. \qquad (17)$$

Here, $h_s = k_{sz}c/\omega_s$, and $\kappa_s = k_{s\perp}c/\omega_s = \sqrt{1-h_s^2}$ are the normalized axial and transverse wave numbers, respectively, I_b is the DC current beam, R_0 is the guiding center radius of electrons in a thin annular electron beam. The quantity ν is the eigenvalue for the TE_{mp} wave [it is the pth root of the equation $J_m'(\nu) = 0$].

Below we consider three symmetric waveguide modes: TE_{01}, TE_{02}, and TE_{03}, resonant at the fundamental, second, and third harmonic of the cyclotron frequency, respectively. Using the derivation procedure detailed in the Appendix, one can obtain from (16) the following simplified equations describing the evolution of the wave amplitudes:

$$\frac{dF_1}{d\xi} = -\frac{I_1}{2\pi}e^{-i\delta_1\xi}\int_0^{2\pi}\frac{p_\perp}{2}e^{-i\varphi}\left[1 + b_2\frac{p_\perp}{2}e^{i\theta} + b_3\frac{p_\perp^2}{8}e^{i2\theta}\right]d\varphi_0, \qquad (18a)$$

$$\frac{dF_2}{d\xi} = -\frac{I_2}{2\pi}\int_0^{2\pi}\frac{p_\perp}{2}e^{-i2\varphi}\left[b_1 e^{-i\theta} + p_\perp + b_3\frac{p_\perp^2}{2}e^{i\theta}\right]d\varphi_0, \qquad (18b)$$

$$\frac{dF_3}{d\xi} = -\frac{I_3}{2\pi}e^{-i\delta_3\xi}\int_0^{2\pi}\frac{p_\perp}{2}e^{-i3\theta\varphi}\left[b_1 e^{-i2\theta} + b_2\frac{3p_\perp}{2}e^{-i\theta} + \frac{9}{8}p_\perp^2\right]d\varphi_0, \qquad (18c)$$

where the Bessel functions have been replaced by their polynomial expansions. The parameters δ_1 and δ_3 account for the departure of the TE_{01} and TE_{03} waves from exact resonance, respectively. These parameters are given by (A5). The phase variable $\varphi = (\omega_2 t - k_{2z}z)/2 - \theta$ is the phase of the wave with respect to the electron gyrophase for the second harmonic resonance ($\theta = \theta_0 + \mu\xi$). So averaging over φ_0 in (18) is equivalent to the averaging over θ_0 in (16).

Equations for the normalized electron energy and phase are similar to those given in Refs. [11] and [19], where the interaction between an electron beam and a single wave was considered:

$$\frac{d\gamma}{d\xi} = \frac{p_\perp}{2}\,\mathrm{Re}\left\{F_1 e^{i(\varphi+\delta_1\xi)}\left[1 + b_2\frac{p_\perp}{2}e^{-i\theta} + b_3\frac{p_\perp^2}{8}e^{-i2\theta}\right] + F_2 e^{i2\varphi}\left[b_1 e^{i\theta} + p_\perp + b_3\frac{p_\perp^2}{2}e^{-i\theta}\right] + F_3 e^{i(3\varphi+\delta_3\xi)}\left[b_1 e^{i2\theta} + b_2\frac{3p_\perp}{2}e^{i\theta} + \frac{9}{8}p_\perp^2\right]\right\}, \tag{19}$$

$$\frac{d\varphi}{d\xi} = \gamma - 1 + \Delta - \mathrm{Re}\left\{iF_1 e^{i(\varphi+\delta_1\xi)}\left[\left(1-\frac{\gamma}{p_\perp^2}\right)\frac{p_\perp}{2} + b_2\left(1-\frac{2\gamma}{p_\perp^2}\right)\frac{p_\perp^2}{8}e^{-i\theta} + b_3\left(1-\frac{3\gamma}{p_\perp^2}\right)\frac{p_\perp^3}{48}e^{-i2\theta}\right] + iF_2 e^{i2\varphi}\left[b_1\left(1-\frac{\gamma}{2p_\perp^2}\right)p_\perp e^{i\theta} + \left(1-\frac{\gamma}{p_\perp^2}\right)\frac{p_\perp^2}{2} + b_3\left(1-\frac{3\gamma}{2p_\perp^2}\right)\frac{p_\perp^3}{6}e^{-i\theta}\right] + iF_3 e^{i(3\varphi+\delta_3\xi)}\left[b_1\left(1-\frac{\gamma}{3p_\perp^2}\right)\frac{3p_\perp}{2}e^{i2\theta} + b_2\left(1-\frac{2\gamma}{3p_\perp^2}\right)\frac{9p_\perp^2}{8}e^{i\theta} + \left(1-\frac{\gamma}{p_\perp^2}\right)\frac{9p_\perp^3}{16}\right]\right\}. \tag{20}$$

Here, γ is the electron energy normalized to its initial value γ_0, and $\Delta = 1 - h_2\beta_{z_0} - \mu$ is the cyclotron resonance detuning or initial synchronism mismatch. In this normalization, electron energy and momentum are related as $\gamma^2 = \gamma_0^{-2} + p_\perp^2 + p_z^2$. Note that in the absence of overlapping of cyclotron resonances, i.e., when $b=0$, the self-consistent Eqs. (18), (19), and (20) are greatly simplified. Then, each wave interacts with the electron beam at a single harmonic.

For the gyro-TWT the boundary conditions for all variables in (18)–(20) are

$$\gamma(0) = 1, \quad \varphi(0) = \omega_s t_0 - \theta_0 = \varphi_0 \in [0, 2\pi), \quad p_\perp(0) = \beta_{\perp_0}. \tag{21}$$

In the case of the gyrotwystron with a single-cavity fundamental harmonic prebunching, the boundary conditions at the entrance of the output waveguide are:

$$\gamma(0) = 1, \quad \varphi(0) = \varphi_0 + q\sin\varphi_0 + \Theta_{dr}, \quad \varphi_0 \in [0, 2\pi), \quad \text{and } F(\xi = 0) = 0, \tag{22}$$

Equations (18)–(20) form a self-consistent set where parameters q and Θ_{dr} are the bunching parameter and electron transit angle through the drift section, respectively. These parameters are defined in [20].

Equations (18) and (19) form a self-consistent set of equations from which follows the energy conservation law:

$$I_1^{-1}(|F_1|^2 - |F_1(0)|^2) + I_2^{-1}(|F_2|^2 - |F_2(0)|^2) + I_3^{-1}(|F_3|^2 - |F_3(0)|^2) = 2(1-\gamma_0^{-1})\eta, \tag{23}$$

where $F_s(0)$ is the initial amplitude of the wave and η is the efficiency of the electron beam-wave interaction,

$$\eta = \frac{(1 - \langle\gamma\rangle)}{(1 - \gamma_0^{-1})}. \tag{24}$$

Here the angular brackets mean averaging over initial phases φ_0.

IV. RESULTS

The set of Eqs. (18)–(20) with corresponding boundary conditions was studied for the case of the absence of resonance overlapping ($b=0$) in the gyro-TWT and the gyrotwystron. An annular beam of radius 0.8 cm, 500 kV, 400 A, and pitch factor $\alpha=1$ was considered. The waveguide radius was 2.1 cm and the RF driver frequency was 9 GHz (the motivations for this choice of parameters will be explained later.) These values of the beam and waveguide parameters correspond to normalized beam currents $I_1=0.045$, $I_2=0.008$, $I_3=0.004$, and frequency mismatch parameters $\delta_1=0.132$, and $\delta_3=-0.098$. The normalized axial wave numbers of the three waves were $h_1=0.25$, $h_2=0.46$, and $h_3=0.51$, respectively. The parameter μ characterizing the external magnetic field, and, correspondingly, the detuning Δ in Eq. (20) was varied in simulations.

A. Gyro-TWT Results

We were interested in the effect of a mode excited initially by a driver on the excitation of two other modes. Two interaction cases described in Sec. I were considered. First, we assumed that an electron beam interacts with the TE_{01} wave at the fundamental cyclotron resonance and studied the effects of this wave on the excitation of the TE_{02} and TE_{03} waves. The magnetic field was optimized for achieving the most efficient interaction between the beam and the TE_{01} wave. The results are presented in Figs. 2(a)–2(d) for the initial normalized field amplitudes $F_1(0)=0.005$, $F_2(0)=0$, $F_3(0)=0$, and the initial cyclotron resonance detuning $\Delta=0$ (recall that $\Delta=1-h_2\beta_{z_0}-\mu$). In Fig. 2(a) the normalized wave intensities are shown as functions of the axial distance. This figure exhibits a significant growth of the high frequency waves. The excitation of the TE_{02} and TE_{03} waves is a typical case of the generation of signal frequency harmonics known in TWT's [15]: the resonance interaction between the TE_{01} wave and the electron beam gives rise to harmonics of the signal frequency in the current density term, which in turn excites the high-order modes. The gain of the TE_{01} wave is shown in Fig. 2(b). This curve does not depend on the other waves because the second and third waves absorb only a small amount of energy from the beam. Figure 2(c) shows the electron phases as a function of the normalized axial waveguide length and Fig. 2(d) shows the position of electrons in the phase space ($p_x=p_\perp\cos\varphi$ and $p_y=p_\perp\sin\varphi$) at

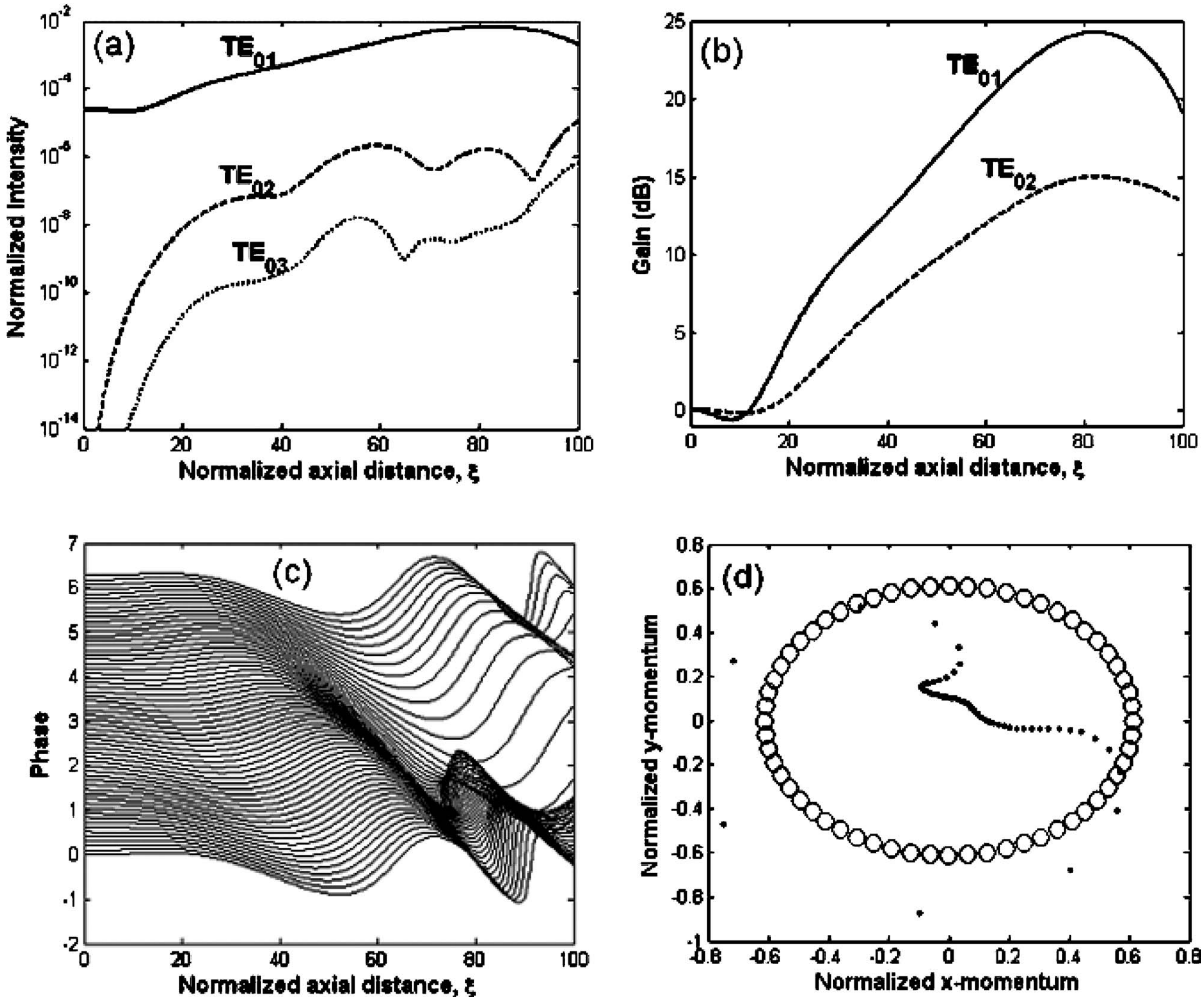

FIG. 2. Operation of the fundamental harmonic gyro-TWT for $b=\Delta=0$: axial dependences of normalized wave intensities (a), gain (b), and electron phases (c). Figure (d) shows electron locations in the phase space of the gyro-TWT at the waveguide entrance ($\xi=0$—circles) and at $\xi=80$ (dots) where the gain and efficiency are maximal ($p_x=p_\perp \cos\varphi$, $p_y=p_\perp \sin\varphi$).

the entrance of the waveguide and at the point of maximum efficiency. From these two figures it is clear that the TE_{01} wave is the dominant mode because a single electron bunch is formed.

In the second case, the electron beam interacts primarily with the TE_{02} wave at the second cyclotron harmonic. The axial dependence of the intensities of all three waves is shown in Fig. 3(a) for initial normalized field amplitudes $F_1(0)=0.0001$, $F_2(0)=0.005$, $F_3(0)=0.0001$, and initial cyclotron resonance detuning $\Delta=0.046$. The normalized intensities of the two waves TE_{01} and TE_{03} can be seen increasing with the axial length, but they remain significantly smaller than the primary wave intensity. The excitation of the neighboring harmonics due to the excitation of the second harmonic wave can be attributed to the nonlinear "four-photon" process described in [21]. The gain curve presented in Fig. 2(b) (dashed line) shows no significant change due to the presence of two other waves. However, the maximum gain is smaller than the value obtained for the fundamental harmonic operation. The phase plot and the electron trajectories presented in Fig. 3(b) and 3(c) show two bunches separated by an angular distance of π. This confirms that the second harmonic TE_{02} mode is the strongest mode in this interaction, because the formation of two electron bunches corresponds to the quadrupole nature of the second harmonic resonance field (see, e.g., Ref. [7]).

B. Gyrotwystron Results

It was assumed that a modulated electron beam interacts primarily with the TE_{01} wave. The magnetic field was optimized so as to achieve the most efficient interaction between the electron beam and the TE_{01} mode. The results are presented in Figures 4(a)–4(c), which show the axial dependence of normalized intensities (a), the interaction efficiency (b), and the electron positions in phase space (c) for $\Delta=-0.03$ and bunching parameter $q=1.5$. In Fig. 4(a) the normalized intensity of each wave is shown for two interaction cases: when the beam interacts with a single wave (solid lines) and when the beam interacts with a wave in the pres-

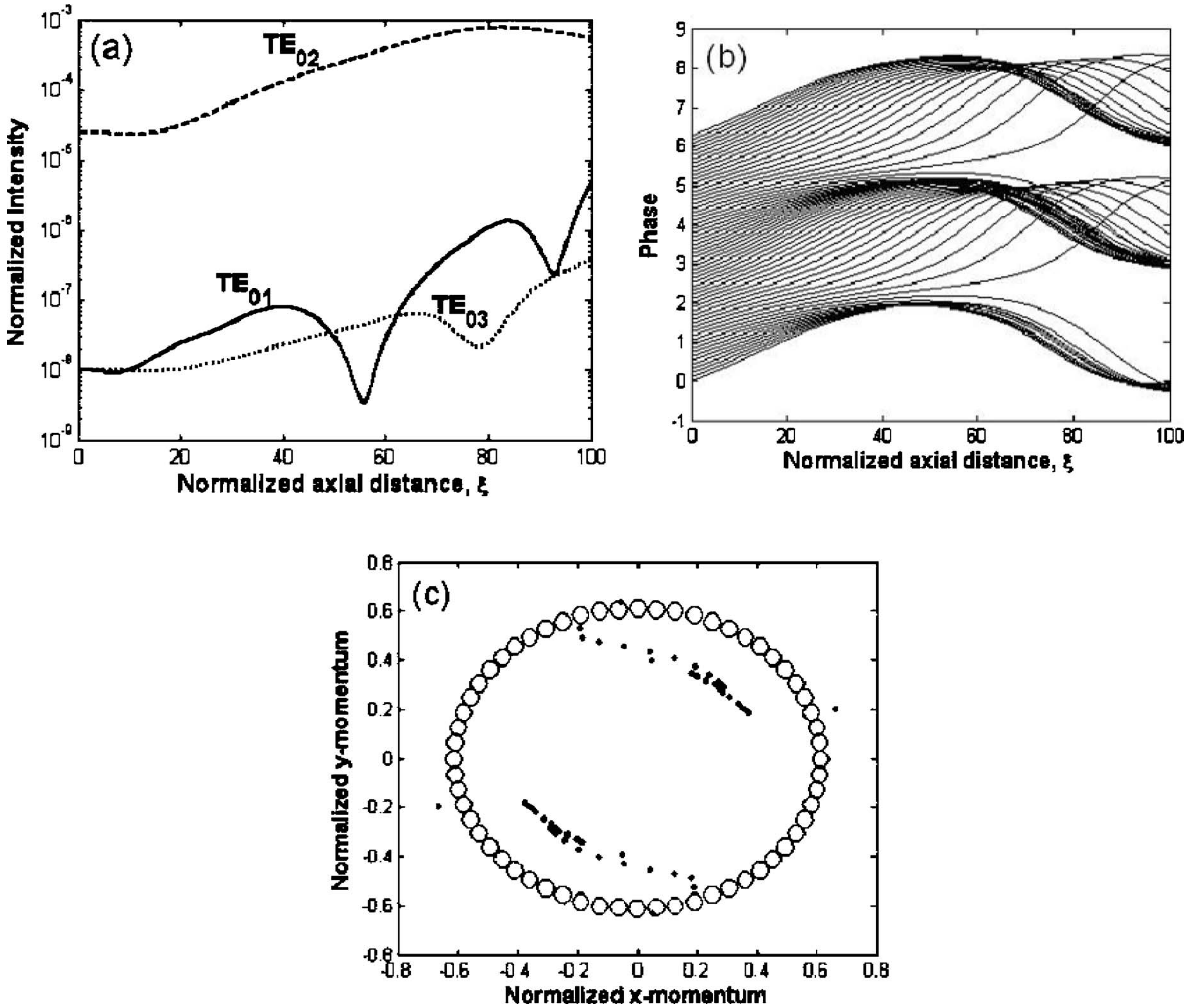

FIG. 3. Operation of the second harmonic gyro-TWT for $b=0$ and $\Delta=0.046$: axial dependences of normalized wave intensities (a), and electron phases (b). Figure (c) shows electron locations in the phase space of the gyro-TWT at the waveguide entrance ($\xi=0$—circles) and at $\xi=80$ (dots) where the gain is maximum ($p_x=p_\perp \cos\varphi$, $p_y=p_\perp \sin\varphi$).

ence of other waves (dashed lines). It is apparent from Fig. 4(a) that the radiation intensity of each wave decreases slightly when the wave interacts with the beam in the presence of other waves (parametric interaction). This can be explained by the fact that each wave extracts some energy from the same beam. The net efficiency of the device is shown in Fig. 4(b) along with the efficiency curves for the case of single wave interaction. It is clear that the net efficiency of the device is a little higher than the efficiency obtained when only the dominant mode (TE_{01}) interacts with the beam. Therefore, the nonlinear excitation of the side modes can slightly improve the net efficiency of the device in this case. In Fig. 4(c) the electrons are shown at the entrance of the waveguide and at $\xi=34$ where the efficiency is maximum. One can see that a single electron bunch at the entrance is formed due to ballistic bunching in the drift space and then this bunch is decelerated.

V. OVERLAPPING OF RESONANCES EFFECTS

In this section we assume that electron beam interacts with each of the waves at the first three cyclotron harmonics simultaneously, i.e., the parameter b in Eqs. (18)–(20) is now nonzero. We present the results for the gyro-TWT and the gyrotwystron separately.

A. Gyro-TWT

Two distinct cases, viz., the dominant TE_{01} and the dominant TE_{02} waves, were again considered. For the first case with $\Delta=0$, the results are shown in Fig. 5(a) as the wave intensities for nonoverlapping ($b=0$—solid lines), and overlapping ($b=0.5$—dashed lines) cyclotron resonances. One can note that while the maximum intensity of each of the waves remains essentially the same, the overlapping of resonances causes significant rippling in the intensity curves of the TE_{02} and TE_{03} waves. The gain curve is similar to the one obtained for $b=0$ and shown in Fig. 2(b) by a solid line. For the second case, when the magnetic field is tuned so as to excite the TE_{02} wave, the results are shown in Fig. 5(b) for $\Delta=0.046$. It is apparent from the normalized intensity plots in Fig. 5(b) that the overlapping of resonances increases the intensity of the TE_{01} and TE_{03} waves insignificantly. The

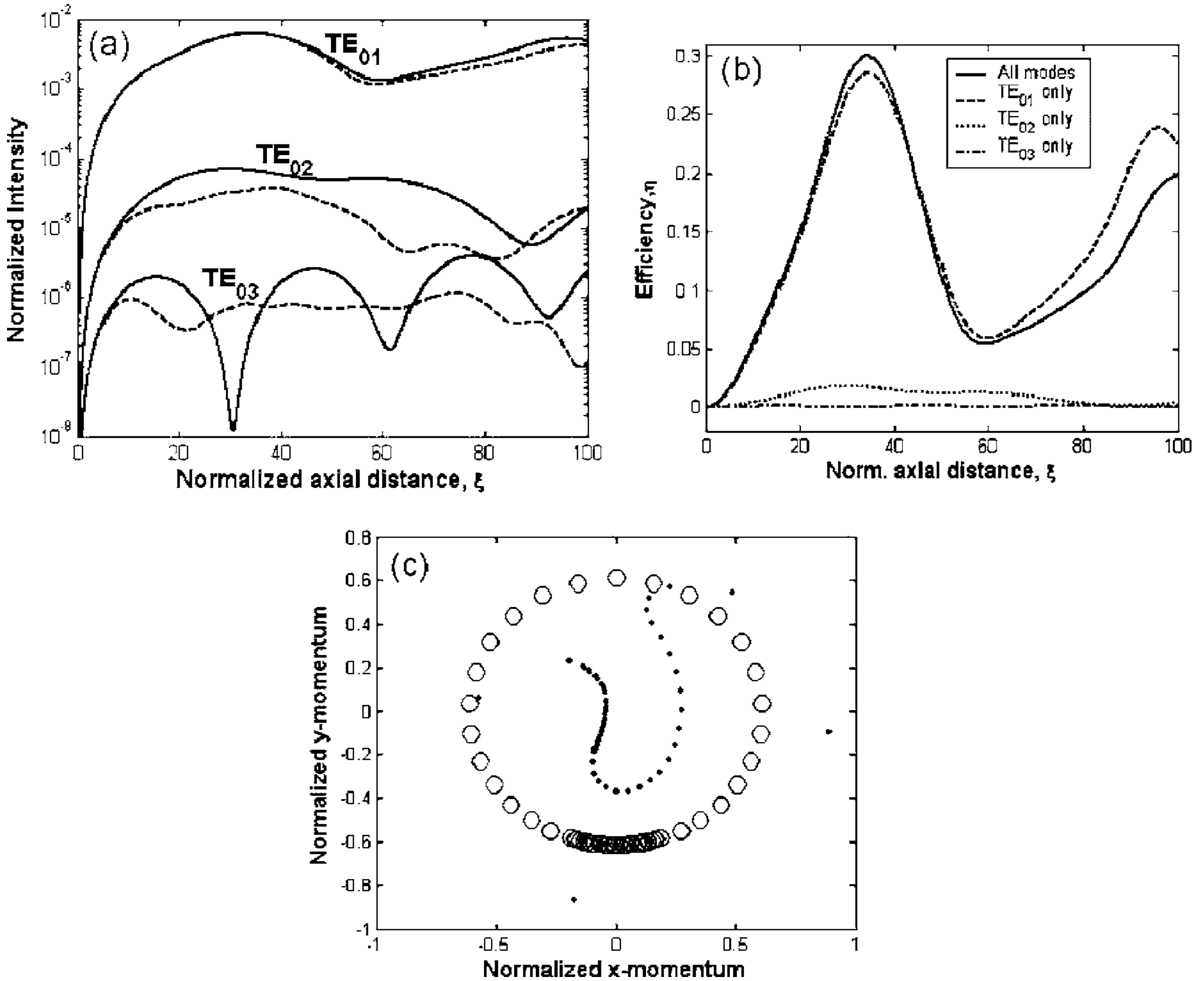

FIG. 4. Parametric interaction (dashed lines) and single wave interaction (solid lines) in the gyrotwystron when $b=0$ and $\Delta=-0.03$: axial dependences of normalized wave intensities (a), and efficiency (b). Figure (c) shows electron position in the phase space of the gyrotwystron at the waveguide entrance ($\xi=0$—circles) and at $\xi=34$ (dots) where the efficiency is maximum.

maximum gain for the case of resonance overlap is the same as the value obtained in the absence of resonances overlap. The curves are similar to those obtained in Fig. 2(b) with the exception that for $b=0.5$ a significant amount of rippling appears.

B. Gyrotwystron

Equations (18)–(20) were studied for the same initial conditions as in Part B of Sec. IV above with $b=0.5$. The results are presented in Figs. 6(a) and 6(b). The normalized wave intensities are shown for the case of single harmonic interaction of the electron beam and waves (solid lines), and for the overlapping of resonances (dashed lines) in Fig. 6(a). The efficiency curves are plotted for both cases in Fig. 6(b). From these figures it is apparent that while the overlapping of resonances does not cause significant changes in the net efficiency of the device, it causes significant rippling in the intensity curves.

VI. DISCUSSION

In the numerical analysis presented above the relativistic beam characteristics were similar to those of the beam used in the relativistic gyrotwystron experiments at the University of Maryland [10]. The relatively high efficiency obtained here (30% compare to 21% obtained in the experiment) can be explained by the fact that we considered a cold beam in our simulations. Maximum efficiency was achieved for a waveguide length of 26 cm in the gyro-TWT and 11 cm in the gyrotwystron for 9 GHz signal frequency. These waveguide length values may give rise to the excitation of parasitic backward waves, which were not taken into account in our analysis.

From numerical results it appears easier to excite high frequency waves when operating at low frequency mode. In the case of operation at the second harmonic, for example, we noticed that the excitation of the first and third waves could not start from noise level, i.e., with $F_1(0)=F_3(0)=0$. Therefore, we did simulations with a small, but nonzero value of $F_{1,3}(0)$. The initial normalized field amplitude of the excited wave, $F(0)=0.005$, corresponds to an input power of about 57 kW for the fundamental cyclotron harmonic resonance operation and 81.4 kW for the case of second harmonic resonance operation. These approximate values were obtained with the use of the following relation [22]:

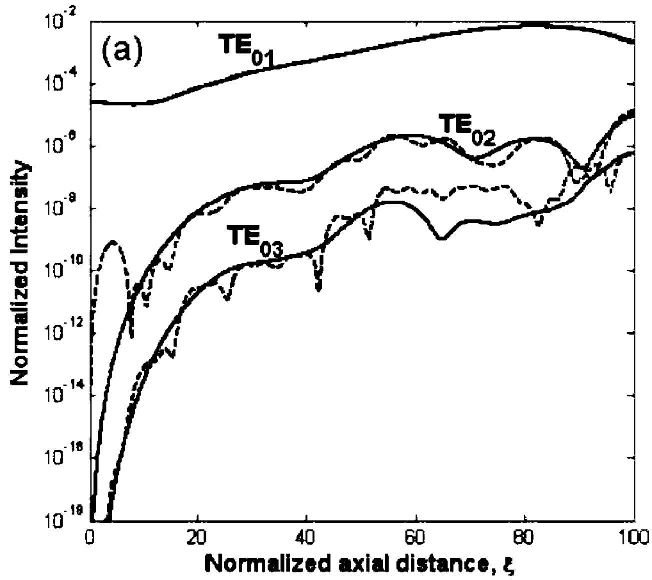

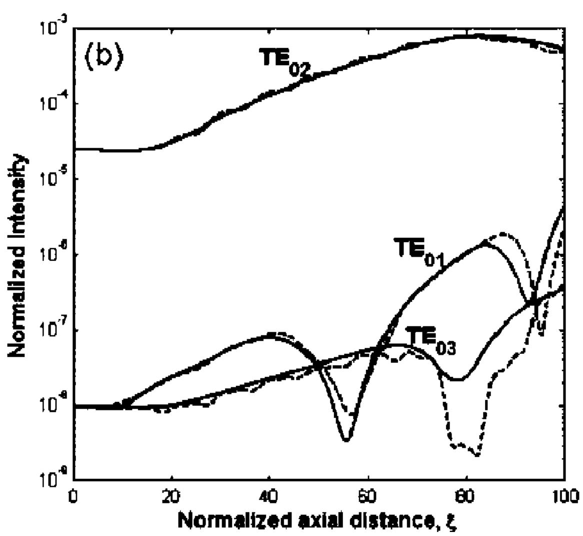

FIG. 5. Effect of the overlapping of cyclotron resonances in the cases of fundamental and second harmonic gyro-TWT operation: axial dependence of normalized wave intensities in the fundamental harmonic gyro-TWT (a) and in the second harmonic gyro-TWT (b) for $b=0$ (solid lines) and $b=0.5$ (dashed lines).

$$F(0) = 0.96 \times 10^{-3} \kappa^2 \sqrt{G_{cpl} P_{in}(kW)/h}. \tag{25}$$

Here, G_{cpl} is the coupling coefficient [cf. Eq. (17)] for an annular beam of radius R_0 interacting with the $TE_{m,p}$ mode of a circular waveguide given by

$$G_{cpl} = \frac{J^2_{m\mp s}(k_\perp R_0)}{(\nu^2 - m^2) J^2_m(\nu)}. \tag{26}$$

The nonlinear excitation of additional waves due to the parametric interaction appears to affect the gyrotwystron performance more than the gyro-TWT performance, certainly, because in the former the waves are excited in the output waveguide by a prebunched electron beam, which already contains harmonics of a signal frequency in its current density spectrum. The overlapping of resonances appears not to

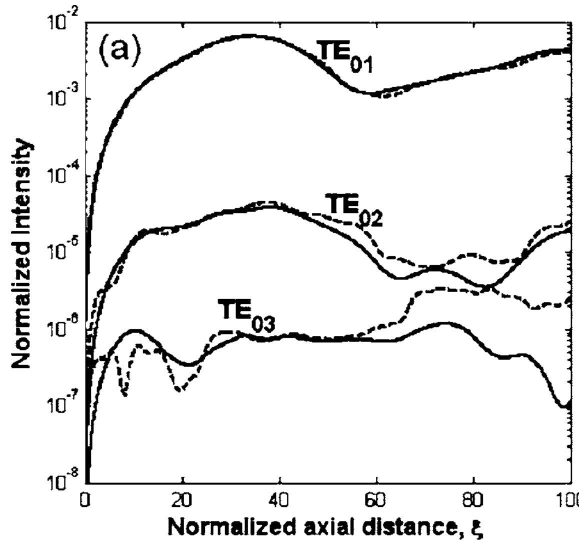

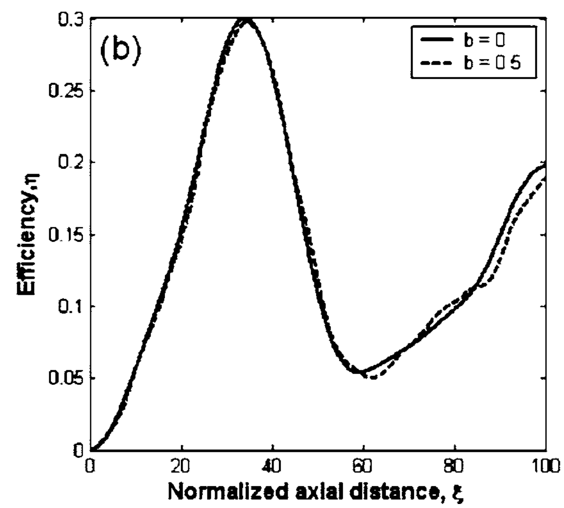

FIG. 6. Effect of the overlapping of cyclotron resonances on the gyrotwystron operation: axial dependences of normalized wave intensities (a), and efficiency (b) for $b=0$ (solid lines) and $b=0.5$ (dashed lines) when $\Delta=-0.03$.

have a significant effect on the performance of the devices.

VII. SUMMARY

In this paper the interaction between three waves at different harmonics of the electron cyclotron frequency in gyro-traveling-wave amplifiers was studied. The paper focused primarily on synchronous waves. It was shown that when an electron beam excites one of the waves, two other waves could be excited through one of two nonlinear interactions similar to the "three-photon" or "four-photon" processes. It was observed that this parametric interaction does not have a significant effect on the net efficiency or gain of the device. It was also noticed that when the overlapping of cyclotron resonances was considered together with parametric interaction the maximum efficiency remained essentially unchanged. This study is relevant to relativistic high power gyro-amplifiers that are being considered as possible drivers for future linear accelerators.

ACKNOWLEDGMENT

This work was supported by the United States Department of Energy Division of High Energy Physics, through Grant No. DEF G 0294 ER 40855.

APPENDIX: DERIVATION OF SIMPLIFIED WAVE EXCITATION EQUATIONS

Let us assume in (16) that the TE_{02} wave interacts with the electron beam at exact cyclotron resonance. Then the electron gyrophase with respect to this wave can be defined as

$$\varphi = (\omega_2 t - k_{2z} z)/2 - \theta. \tag{A1}$$

The electron gyrophase with respect to the TE_{01} and TE_{03} waves can be expressed in terms of φ as follows:

$$\begin{aligned}\omega_1 - k_{1z}z - \theta &= \varphi + (k_{2z}/2 - k_{1z})z\\ &= \varphi + \beta_{z0}\left\{\sqrt{1-\left(\frac{\nu_{02}}{2\hat{R}}\right)^2} - \sqrt{1-\left(\frac{\nu_{01}}{\hat{R}}\right)^2}\right\}\xi,\end{aligned} \tag{A2}$$

$$\begin{aligned}\omega_3 - k_{3z}z - 3\theta &= 3\varphi + (3k_{2z}/2 - k_{3z})z\\ &= 3\varphi + 3\beta_{z0}\left\{\sqrt{1-\left(\frac{\nu_{02}}{2\hat{R}}\right)^2}\right.\\ &\quad\left.-\sqrt{1-\left(\frac{\nu_{03}}{3\hat{R}}\right)^2}\right\}\xi,\end{aligned} \tag{A3}$$

where $\hat{R}=\omega_1 R_W/c$ is the normalized waveguide wall radius, ν_{01}, and ν_{03} are the TE_{01} and TE_{03} waves eigenvalues, respectively. Substituting (A1) and (A3) into (16) we have

$$\begin{aligned}\frac{\partial F_1}{\partial \xi} + \frac{1}{\beta_{gr1}}\frac{\partial F_1}{\partial t'} &= -I_1\frac{1}{2\pi}\int_0^{2\pi} p_\perp e^{-i(\varphi+\delta_1\xi)}[J_1'(\hat{a}_1)\\ &\quad + b_1 J_2'(\hat{a}_1)e^{i\theta} + b_2 J_3'(\hat{a}_1)e^{i2\theta}]d\varphi_0,\end{aligned} \tag{A4a}$$

$$\begin{aligned}\frac{\partial F_2}{\partial \xi} + \frac{1}{\beta_{gr2}}\frac{\partial F_2}{\partial t'} &= -I_2\frac{1}{2\pi}\int_0^{2\pi} p_\perp e^{-i2\varphi}[b_1 J_1'(\hat{a}_2)e^{-i\theta}\\ &\quad + J_2'(\hat{a}_2) + b_2 J_3'(\hat{a}_2)e^{i\theta}]d\varphi_0,\end{aligned} \tag{A4b}$$

$$\begin{aligned}\frac{\partial F_3}{\partial \xi} + \frac{1}{\beta_{gr3}}\frac{\partial F_3}{\partial t'} &= -I_3\frac{1}{2\pi}\int_0^{2\pi} p_\perp e^{-i(3\varphi+\delta_3\xi)}[b_1 J_1'(\hat{a}_3)e^{-i2\theta}\\ &\quad + b_2 J_2'(\hat{a}_3)e^{-i\theta} + J_3'(\hat{a}_3)]d\varphi_0,\end{aligned} \tag{A4c}$$

where

$$\begin{aligned}\delta_1 &= \beta_{z0}\left\{\sqrt{1-\left(\frac{\nu_{02}}{2\hat{R}}\right)^2} - \sqrt{1-\left(\frac{\nu_{01}}{\hat{R}}\right)^2}\right\} \quad \text{and}\\ \delta_3 &= 3\beta_{z0}\left\{\sqrt{1-\left(\frac{\nu_{02}}{2\hat{R}}\right)^2} - \sqrt{1-\left(\frac{\nu_{03}}{3\hat{R}}\right)^2}\right\}.\end{aligned} \tag{A5}$$

If we perform the following change of variable

$$\tau = \left(t' - \frac{\xi}{\beta_{z_0}}\right)\left(\frac{1}{\beta_{gr}} - \frac{1}{\beta_{z_0}}\right)^{-1}, \tag{A6}$$

and replace the Bessel functions $J_s'(\hat{a})$, by their polynomial expansion $\left[J_s(x) \simeq \frac{1}{s!}\left(\frac{x}{2}\right)^s\right]$, Eqs. (A4) can be reduced to the following:

$$\begin{aligned}\frac{\partial F_1}{\partial \xi} + \frac{1}{\beta_{gr1}}\frac{\partial F_1}{\partial t'} &= -\frac{I_1}{2\pi}e^{-i\delta_1\xi}\int_0^{2\pi}\frac{p_\perp}{2}e^{-i\varphi}\left[1 + b_1\frac{p_\perp}{2}e^{i\theta}\right.\\ &\quad\left. + b_2\frac{p_\perp^2}{8}e^{i2\theta}\right]d\varphi_0,\end{aligned} \tag{A7a}$$

$$\begin{aligned}\frac{\partial F_2}{\partial \xi} + \frac{1}{\beta_{gr2}}\frac{\partial F_2}{\partial t'} &= -\frac{I_2}{2\pi}\int_0^{2\pi}\frac{p_\perp}{2}e^{-i2\varphi}\left[b_1 e^{-i\theta} + p_\perp\right.\\ &\quad\left. + b_2\frac{p_\perp^2}{2}e^{i\theta}\right]d\varphi_0,\end{aligned} \tag{A7b}$$

$$\begin{aligned}\frac{\partial F_3}{\partial \xi} + \frac{1}{\beta_{gr3}}\frac{\partial F_3}{\partial t'} &= -\frac{I_3}{2\pi}e^{-i\delta_3\xi}\int_0^{2\pi}\frac{p_\perp}{2}e^{-i3\varphi}\left[b_1 e^{-i2\theta}\right.\\ &\quad\left. + b_2\frac{3p_\perp}{2}e^{-i\theta} + \frac{9}{8}p_\perp^2\right]d\varphi_0.\end{aligned} \tag{A7c}$$

Using the following independent variable for the wave characteristic

$$u = \tau - \xi, \tag{A8}$$

the time dependence of the field amplitude $F_s(\xi,\tau) \to F_s(\xi,u)$ can be eliminated

$$\frac{\partial F_s}{\partial \xi} + \frac{\partial F_s}{\partial \tau} = \frac{\partial F_s}{\partial \xi}. \tag{A9}$$

Correspondingly, Eqs. (A7) reduce to (18).

[1] B. B. Kadomtsev, *Collective Phenomena in Plasmas* (Pergamon Press, 1982).

[2] R. C. Davidson, *Methods in Nonlinear Plasma Theory* (Academic Press, New York, 1972).

[3] A. Yariv, *Quantum Electronics* (John Wiley & Sons, New York, 1975).

[4] N. Blombergen, *Nonlinear Optics* (Benjamin, New York, 1965).

[5] W. H. Louisell, *Coupled Mode and Parametric Electronics* (John Wiley & Sons, New York, 1960).

[6] K. R. Chu, Rev. Mod. Phys. **76**, 489 (2004).

[7] G. S. Nusinovich, *Introduction to the Physics of Gyrotrons* (The Johns Hopkins University Press, Baltimore, 2004).

[8] G. S. Nusinovich, Int. J. Electron. **51**, 457 (1981).

[9] A. V. Gaponov, M. I. Petelin, and V. K. Yulpatov, Radiophys. Quantum Electron. **10**, 794 (1967).

[10] V. L. Granatstein and W. Lawson, IEEE Trans. Plasma Sci. **24**, 648 (1996).

[11] G. S. Nusinovich, R. Ngogang, T. M. Antonsen, Jr., and V. L. Granatstein, Phys. Rev. Lett. **93**, 055101 (2004).

[12] G. S. Nusinovich, Int. J. Electron. **72**, 795 (1992).

[13] G. P. Saraph, T. M. Antonsen, Jr., G. S. Nusinovich, and B. Levush, Phys. Plasmas **2**, 2839 (1995).

[14] W. E. Lamb, Jr., Phys. Rev. **134**, 1429 (1964).

[15] A. S. Gilmour, Jr., *Principles of Traveling Wave Tubes* (Artech House, Boston, 1994).

[16] J. M. Wersinger, J. M. Finn, and E. Ott, Phys. Rev. Lett. **44**, 453 (1980); Phys. Fluids **23**, 1142 (1980).

[17] N. S. Ginzburg, G. S. Nusinovich, and N. A. Zavolsky, Int. J. Electron. **61**, 881 (1986).

[18] M. I. Petelin and V. K. Yulpatov, Radiophys. Quantum Electron. **18**, 212 (1975).

[19] G. S. Nusinovich, P. E. Latham, and O. Dumbrajs, Phys. Rev. E **52**, 998 (1995).

[20] G. S. Nusinovich and H. Li, Phys. Fluids B **4**, 1058 (1992).

[21] G. P. Saraph, T. M. Antonsen, Jr., G. S. Nusinovich, and B. Levush, Phys. Fluids B **5**, 4473 (1993).

[22] G. S. Nusinovich and M. Walter, Phys. Plasmas **4**, 3394 (1997).